



Ultramicroscopy 64 (1996) 99-107

A simple intuitive theory for electron diffraction

D. Van Dyck *, M. Op de Beeck

Department of Physics, University of Antwerp (RUCA), Groenenborgerlaan 171, B-2020 Antwerpen, Belgium

Received 27 October 1995

Abstract

It is shown that the dynamical diffraction can simply be described in real space using the property that electrons are trapped in the electrostatic potential of the atomic columns. Due to this channelling effect, the electron diffraction can be highly dynamical inside each column, and at the same time retain a one-to-one relationship with the crystal structure. This description does not require the crystal to be periodic. Influence of adjacent columns can be treated using a perturbation theory. If the crystal is sufficiently thin, i.e. of the order of 10 nm, and the accelerating voltage is not too high (e.g. 100-300 keV), the motion of the electrons is almost perfectly periodic with depth. The theory shows how the depth periodicity is related to the mass/thickness of the column which allows the exit wavefunction to be parametrized in a simple analytical form. These results open perspectives to solve the inverse problem of how to derive the projected structure of the object from the exit wavefunction.

1. Introduction

Dynamical electron diffraction in perfect crystals is usually described either in terms of Bloch waves or by a slice formalism. Both approaches are very appropriate when the unit cell of the crystal unit cell is small so that only a limited number of diffraction beams is excited. When the crystal unit cell is large or even aperiodic (as for crystal defects) the number of beams may become so large that not only the computation becomes unfeasible but that the physical insight in the theory is lost, certainly since the (weak) phase object approximation is not valid for the object thicknesses that are usually encountered in most experimental conditions. On the other hand, high resolution images show, even for complicated crystals, oriented along a simple zone axis a corre-

There is need for a simple intuitive theory that is valid for larger crystal thicknesses. In our view, a channelling theory fulfils this need. Indeed, it is well known that, when a crystal is viewed along a zone axis, i.e. parallel to the atom columns, the high resolution images often show a one-to-one correspondence with the configuration of columns provided the distance between the columns is large enough and the resolution of the instrument is sufficient. This is for instance the case in ordered alloys with a column structure [1,2]. From this, it can be suggested that, for a crystal viewed along a zone axis with sufficient separation between the columns, the wavefunction at the exit face mainly depends on the projected structure, i.e. on the type of atom columns. Hence, the classical picture of electrons traversing

spondence with the projected structure of the crystal. This effect is difficult to explain using a many-beam description in reciprocal space.

^{*} Corresponding author. Fax: +32 3 218 0257.

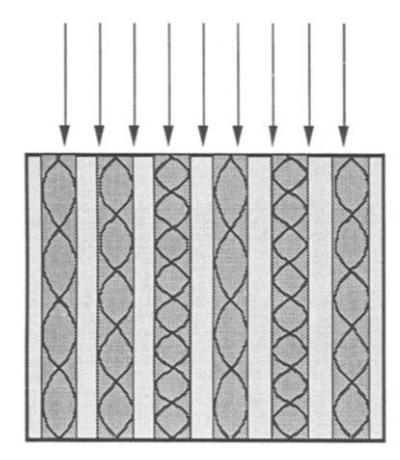


Fig. 1. Schematical representation of highly dynamical 1S electron channelling in an atomic column.

the crystal as plane-like waves in the directions of the Bragg beams which stems from the X-ray diffraction picture and upon which most of the simulation programs are based, is in fact misleading. The physical reason for this "local" dynamical diffraction is the channelling of the electrons along the atom columns parallel to the beam direction. Due to the positive electrostatic potential of the atoms, a column acts as a guide or channel for the electron [3] within which electrons can scatter dynamically without leaving the column (Fig. 1). It has been proposed [5] to exploit this so-called atom column approximation to speed up the dynamical diffraction calculations by assembling the wavefunction at the exit face using parts that have been calculated for each atom column separately. Channelling has been studied intensively in the past (e.g. [4,6,7]).

However, the importance of channelling for interpreting high resolution images has often been ignored or underestimated, probably because of the fact that for historical reasons, dynamical electron diffraction is often described in reciprocal space. However, since most of the high resolution images of crystals are taken in a zone axis orientation, in which the projected structure is the simplest, but in which the number of diffracted beams is the largest, we believe that a simple real-space channelling theory yields a much more useful and intuitive, albeit approximate, description of the dynamical diffraction, which allows us to provide an intuitive interpretation of high resolution images, even for thicker

objects. In [7] the relation between high resolution images and electron channelling has been proposed using a Bloch wave approach. In this work we simplified the theory for channelling in isolated columns.

2. Theory

If we assume that the fast electron, in the direction of propagation (z-axis) behaves as a classical particle with velocity v = hk/m we can consider the z-axis as a time axis with

$$t = mz/hk. (1)$$

Hence we can start from the time-dependent Schrödinger equation

$$-\frac{\hbar}{i}\frac{\partial}{\partial t}\Psi(\mathbf{R},t) = H\Psi(\mathbf{R},t), \qquad (2)$$

with

$$H = -\frac{\hbar^2}{2m} \Delta_R - eU(R, t), \qquad (3)$$

where $U(\mathbf{R},t)$ is the electrostatic crystal potential, m and k the relativistic electron mass and inverse wavelength and $\Delta_{\mathbf{R}}$ the Laplacian operator acting in the plane (\mathbf{R}) perpendicular to z. Using (1) we then have

$$\frac{\partial}{\partial z} \Psi(\mathbf{R}, t) = \frac{i}{4\pi k} (\Delta_{\mathbf{R}} + V(\mathbf{R}, z)) \Psi(\mathbf{R}, t), \quad (4)$$

with

$$V(\mathbf{R},z) = \frac{2me}{\hbar^2} U(\mathbf{R},z). \tag{5}$$

This is the well-known high energy equation in real space which can also be derived from the stationary Schrödinger equation in the forward scattering approximation [3].

The solution of (4) can be expanded in eigenfunctions of the Hamiltonian

$$\Psi(\mathbf{R},z) = \sum_{n} C_{n} \Phi_{n}(\mathbf{R}) \exp\left\{-i\pi \frac{E_{n}}{E_{o}} kz\right\}, \qquad (6)$$

with H given by (3) and

$$E_{\rm o} = \frac{h^2 k^2}{2m} \tag{7}$$

is the incident electron energy, λ the electron wavelength. For $E_n < 0$ the states are bound to the columns. We now rewrite (6) as

$$\Psi(\mathbf{R}, z) = \sum_{n} C_{n} \Phi_{n}(\mathbf{R}) \left[1 - i\pi \frac{E_{n}}{E_{o}} kz \right]$$

$$+ \sum_{n} C_{n} \Phi_{n}(\mathbf{R}) \left[\exp \left\{ -i\pi \frac{E_{n}}{E_{o}} kz \right\} \right]$$

$$- 1 + i\pi \frac{E_{n}}{E_{o}} kz \right].$$
 (8)

The coefficients C_n are determined from the boundary condition

$$\sum_{n} C_{n} \Phi_{n}(\mathbf{R}) = \Psi(\mathbf{R}, 0), \qquad (9)$$

from which

$$C_{n} = \int \Phi_{n}^{*}(\mathbf{R}) \Psi(\mathbf{R},0) \, \mathrm{d}\mathbf{R}. \tag{10}$$

In case of plane wave incidence one thus has

$$\sum_{n} C_{n} \Phi_{n}(\mathbf{R}) = 1, \tag{11}$$

and from (3), (9) and (11)

$$\sum_{n} C_n E_n \Phi_n(\mathbf{R}) = H \Psi(\mathbf{R}, 0) = -eU(\mathbf{R}), \qquad (12)$$

where from now on the projected potential is assumed. Now (8) becomes

$$\Psi(\mathbf{R},z) = 1 + i\pi \frac{eU(\mathbf{R})}{E_o} kz + \sum_n C_n \Phi_n(\mathbf{R})$$

$$\times \left[\exp\left\{ -i\pi \frac{E_n}{E_o} kz \right\} - 1 + i\pi \frac{E_n}{E_o} kz \right]. \tag{13}$$

The first two terms yield the well-known weak phase object approximation. In the third term only those states will appear in the summation for which

$$|E_n| \ge E_0 / kz. \tag{14}$$

In case the object is very thin, so that no state obeys (14), the weak phase object approximation is valid. For a thicker object, only bound states will appear

with very deep energy levels, which are localised near the column cores. Furthermore, a two-dimensional projected column potential has only very few deep states, and when the overlap between adjacent columns is small only the radial symmetric states will be excited. In practice, for most types of atom columns, only one state appears, which can be compared with the 1S state of an atom.

In the case of an isolated column, taking the origin in the centre of the column, we then have

$$\Psi(\mathbf{R}, z) = 1 + i\pi \frac{eU(\mathbf{R})}{E_o} kz + C\Phi(\mathbf{R}) \left[\exp\left\{ -i\pi \frac{E}{E_o} kz \right\} - 1 + i\pi \frac{E}{E_o} kz \right].$$

A very interesting consequence of this description is that, since the state Φ is very localised at the atom core, the wavefunction for the total crystal can be expressed as a superposition of the individual column functions

$$\Psi(\mathbf{R},z) = 1 + i\pi \frac{eU(\mathbf{R})}{E_o} kz + \sum_i C_i \Phi_i(\mathbf{R} - \mathbf{R}_i)$$

$$\times \left[\exp\left\{ -i\pi \frac{E_i}{E_o} kz \right\} - 1 + i\pi \frac{E_i}{E_o} kz \right],$$
(16)

with

$$U(\mathbf{R}) = \sum_{i} U_{i}(\mathbf{R} - \mathbf{R}_{i}). \tag{17}$$

If all the states other than the Φ_i have very small energies, i.e.

$$|E_i| \ll E_o/kz,\tag{18}$$

then (8) can be simplified as

$$\Psi(\mathbf{R},z) = \sum_{n} C_{n} \Phi_{n}(\mathbf{R}) + \sum_{n} C_{n} \Phi_{n}(\mathbf{R})$$

$$\times \left[\exp \left\{ -i\pi \frac{E_{n}}{E_{o}} kz \right\} - 1 \right], \tag{19}$$

so that (15) becomes

$$\Psi(\mathbf{R},z) = 1 + C_i \Phi_i (\mathbf{R} - \mathbf{R}_i)$$

$$\times \left[\exp \left\{ -i \pi \frac{E_i}{E_o} kz \right\} - 1 \right], \tag{20}$$

and (16) becomes

$$\Psi(\mathbf{R}, z) = 1 + \sum_{i} C_{i} \Phi_{i} (\mathbf{R} - \mathbf{R}_{i})$$

$$\times \left[\exp \left\{ -i\pi \frac{E_{i}}{E_{0}} kz \right\} - 1 \right]. \tag{21}$$

Expressions (16) and (21) are the basic result of this channelling theory.

The interpretation of (21) is simple. Each column i acts as a channel in which the wavefunction oscillates periodically with depth. The periodicity is related to the "weight" of the column, i.e. proportional to the atomic number of the atoms in the column and inversely proportional to their distance along the column. The importance of these results lies in the fact that they describe the dynamical diffraction for larger thicknesses than the usual phase grating approximation and that they require only the knowledge of one function Φ_i per column (which can be tabulated similar to atom scattering factors or potentials). Furthermore, even in the presence of dynamical scattering, the wavefunction at the exit face still retains a one-to-one relation with the configuration of columns. Hence this description is very useful for interpreting high resolution images and to provide a possible answer to the direct retrieval problem. Eq. (21) applies to light columns, such as Si(111) or Cu(100) with an accelerating voltage up to about 200 keV. When the atom columns are "heavier" and the accelerating voltage is higher (which due to the relativistic correction also increases the effective strength of the potential) then (16) has to be used. This is for example the case for Au(100).

Fig. 2 shows the electron density $|\Psi(R,z)|^2$ as a function of depth in a Au₄Mn alloy crystal for 200 keV incident electrons. The corners represent the projection of the Mn column. The square in the centre represents the four Au columns. The distance between adjacent columns is 0.2 nm. The periodicity along the direction of the column is 0.4 nm. From

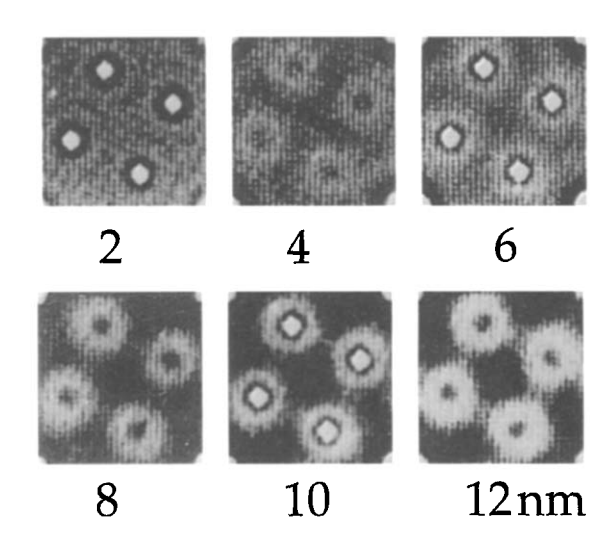


Fig. 2. The electron density at the exit plane of Au₄Mn crystals of different thickness, calculated with a multi-slice based simulation program.

these results it is clear that the electron density in each column fluctuates nearly periodically with depth. For Au this periodicity is about 4 nm and for Mn 13 nm. These periodicities are nearly the same as for isolated columns so that the influence of neighbouring columns in this case is still small. The energies of the respective s states are respectively about 250 and 80 eV.

When the atoms are heavy and the accelerating voltage very high (0.5 to 1 MeV), a larger number of states come in and the result becomes more complicated. When the crystal is viewed along a higher index zone axis, the distance between adjacent columns decreases whereas the weight of the columns also decreases. Hence the bound states broaden and overlap between adjacent columns starts to occur. This can be incorporated in the theory using perturbation theory. When the overlap between columns is too large one has to consider them as a kind of molecules [5]. The localisation can also be improved by using higher voltages. It has to be stressed that the derived results are only valid in a perfect zone axis orientation. A slight tilt can destroy the symmetry and excite other, non-symmetric states, so that the results become much more complicated. It is interesting to note that channelling has usually been described in terms of Bloch waves [6,7]. However as follows from the foregoing, channelling is not a mere

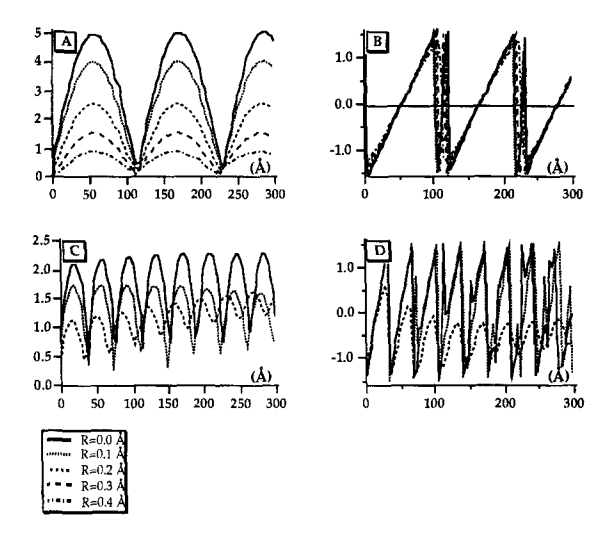


Fig. 3. (A, B) Amplitude and phase of the wavefunction " $\Psi - 1$ " as a function of the thickness for an isolated Cu column (multislice, 200 kV). (C, D) Amplitude and phase of the wavefunction " $\Psi - 1$ " as a function of the thickness for an isolated Au column (multi-slice, 200 kV).

consequence of the periodicity of the crystal but occurs even in an isolated column parallel to the beam direction. In fact, even for an isolated column, the problem can be treated mathematically by making the column artificially periodical so as to generate a basis of functions (Bloch functions) to expand the wavefunction. In this view, the Bloch character is

only of mathematical importance. Even in a crystal in which the distance between the adjacent columns is sufficient (e.g. 0.2 nm), this is the case. Bloch wave calculations then yield the same 1S states as found in our simplified treatment. Only when the overlap between columns increases or when the beam is inclined, the other Bloch states do become physically important.

3. Test of the validity

In order to test the validity of the theory, we compared the theoretical results with simulations using a real-space slice program. In case of one single column of type i, centred at the origin, one expects, from (20), in case the column is not too heavy.

$$\Psi(\mathbf{R},z) - 1 = 2\Phi_{i}(\mathbf{R}) \sin\left\{\frac{\pi E_{i}}{2E_{o}}kz\right\} \exp\left\{-i\left[\frac{\pi}{2} + \frac{\pi E_{i}}{2E_{o}}kz\right]\right\},$$
 (22)

i e

• the amplitude decreases with increasing distance R from the centre of the columns with a slope given by $\Phi_i(R)$, the 1S eigenfunction;

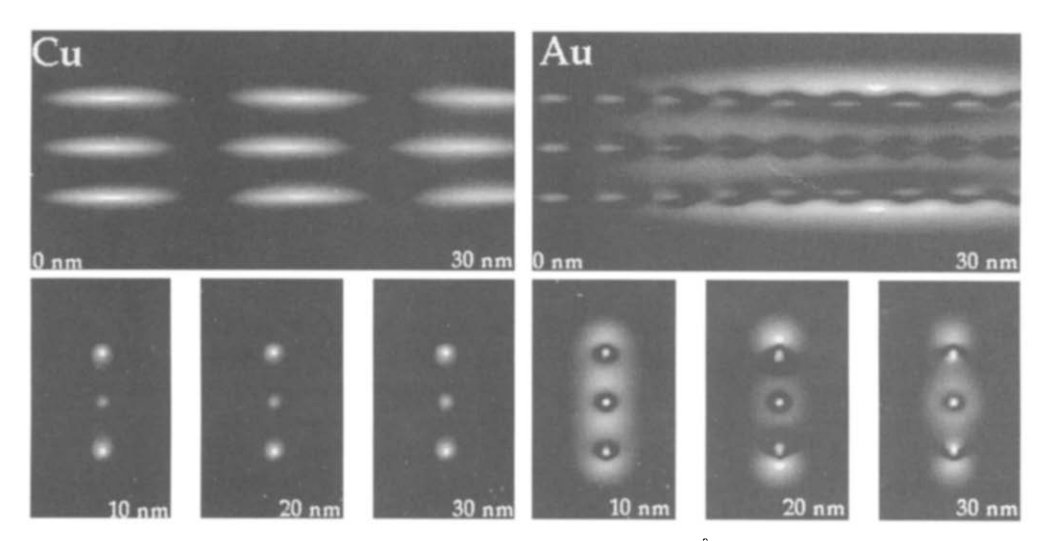


Fig. 4. The intensity of the wavefunction " Ψ -1" for an artificial unit cell of $(5 \times 4 \times 4 \text{ Å})$ consisting of three Cu (or Au) columns with an inter-atomic distance of 1 Å. (Top) Side view. (Bottom) Top view.

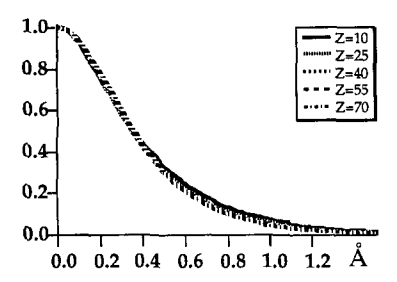


Fig. 5. The scaled eigenstate $\phi(R)$ as a function of \sqrt{E} for various atomic mass Z, calculated from the channelling eigenvalue problem.

- the amplitude oscillates with depth with a periodicity of 4E₀/kE_i;
- the phase increases linearly with depth, starting from $-\pi/2$.

Fig. 3 shows the amplitude (A) and phase (B) of $(\Psi-1)$ for one isolated Cu column, with periodicity 3.8 Å along the ordered axis. These results are in complete agreement with (22). Fig. 3 (C and D) show the amplitude and phase for an isolated heavier column of Au with repeat distance of 4.08 Å along the column. Here the oscillation of the amplitude is superimposed onto a linearly increasing function. This is in agreement with the improved expression (15).

In order to demonstrate the validity of the theory when the columns are very close we performed a simulation of $|\Psi - 1|^2$ for an artificial unit cell $(5 \times 4 \times 4 \text{ Å})$ consisting of three Cu (or Au) columns with an artificial distance of 1 Å (Fig. 4). It is clear

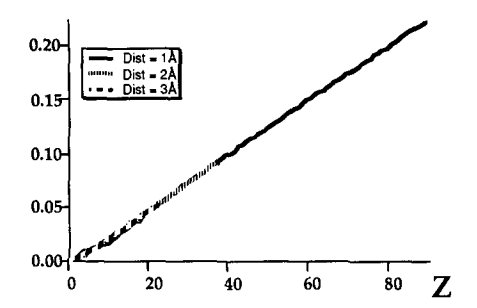


Fig. 6. The linear scaling of the energy E as a function of $Z/d^{5/4}$, calculated from the channelling eigenvalue problem.

that the periodicity, as expected for an isolated column, holds for Cu up to a thickness of 30 nm and for Au up to 10 nm.

4. Universal scaling

As is clear from Figs. 5 and 6 the eigenfunctions empirically seem to scale with \sqrt{E} and the eigenenergy E scales with $Z/d^{5/4}$ with Z the atomic charge and d the distance between the atoms in the column. This scaling behaviour allows us to parametrize the wavefunction in the form:

$$\Psi(\mathbf{R}, z) = 1 + \alpha \left[\exp \left\{ -i\pi \frac{E}{E_o} kz \right\} - 1 \right]$$

$$\times E^{-1/2} \Phi_o(\sqrt{E} \mathbf{R}). \tag{23}$$

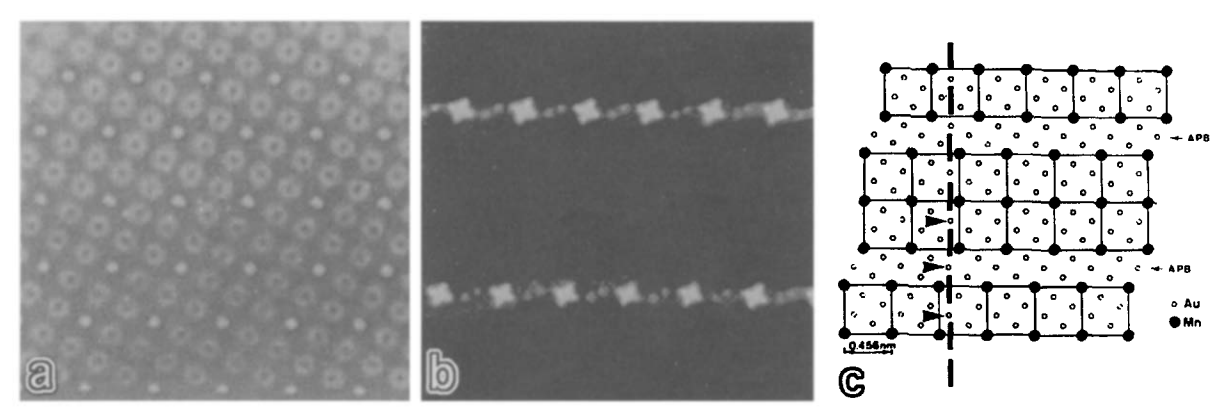


Fig. 7. Deviation from the ideal channelling at the translation interface in Au_4Mn (see text), calculated with a multi-slice simulation program. (a) Electron density at the exit phase. (b) Different image. (c) Model.

This expression can still be improved so as to hold for thicker objects and/or heavier columns:

$$\Psi(\mathbf{R},z) = 1 + \beta E^{4/5} V_{o}(\mathbf{R}) + \alpha \left[\exp \left\{ -i\pi \frac{E}{E_{o}} kz \right\} - 1 + i\pi \frac{E}{E_{o}} kz \right] \times E^{-1/2} \Phi_{o}(\sqrt{E} \mathbf{R}),$$
(24)

where $V_{\rm o}$ and $\Phi_{\rm o}$ are universally scaled functions for the projected potential and the 1S bound state, respectively, while α and β are proper constant excitation factors. The advantage of this result is that the exit wavefunction is expressed analytically in terms of the parameters (Z, d, z, column position) that describe the crystal structure. This result enables us to calculate image and diffraction patterns in an analytical (and thus very fast way) and also to solve the inverse problem of deriving the crystal structure by fitting with the experimentally reconstructed object wave.

5. Discussion

5.1. Channelling and defects

The channelling effect still occurs in the presence of defects such as translation interfaces, twin interfaces, dislocations, provided the columns parallel to the incident beam are not disrupted. To demonstrate this we take again the Au, Mn alloy of Fig. 2 in which we now introduce translation interfaces (antiphase boundaries) (Fig. 7 right). The electron density, calculated with the periodic continuation method is shown in the centre (thickness 8 nm). If the channelling along the individual columns would not be affected by the interface, the electron density at both sides of the interface would be identical to that of the perfect crystal shifted over the displacement vector of the interface. In order to reveal the deviation from this ideal situation, we subtract this "ideal" electron density at both sides and display the difference with increased contrast (Fig. 7 middle) [11]. From this it is clear that the deviation from the ideal channelling condition is very small and occurs only very close to the interface.

5.2. Diffraction pattern

Fourier transforming the wavefunction (21) at the exit face of the object yields the wavefunction in the diffraction plane, which can be written as

$$\Psi(\mathbf{g},z) = \delta(\mathbf{g}) + \sum_{i} F_{i}(\mathbf{g},z) \exp\{-i2\pi\mathbf{g} \cdot \mathbf{R}_{i}\}$$
(25)

(in the case of heavy columns we will have to use (16) instead). In a sense the simple kinematical expression for the diffraction amplitude holds, provided the scattering factor for the atoms is replaced by a dynamical scattering factor for the columns, in a sense as obtained in [8] and which is defined by

$$F_i(\mathbf{g}, z) = \left[\exp \left\{ -i\pi \frac{E}{E_o} kz \right\} - 1 \right] C_i f_i(\mathbf{g}), \quad (26)$$

with $f_i(\mathbf{g})$ the Fourier transform of $\Phi_i(\mathbf{R})$. It is clear that the dynamical scattering factor varies periodically with depth. This periodicity may be different for different columns.

In case of a monatomic crystal, all F_i are identical. Hence $\Psi(\mathbf{g},z)$ varies perfectly periodically with depth. In a sense the electrons are periodically transferred from the central beam to the diffracted beams and back. The periodicity of this dynamical oscillation (which can be compared with the Pendellösung effect) is called the dynamical extinction distance. It has for instance been observed in Si(111). An important consequence of (21) is the fact that the diffraction pattern can still be described by a kinematical type of expression so that existing results and techniques that have been based on the kinematical theory remain valid to some extent for thicker crystals in zone axis orientation. Examples are

- diffraction at periodical stacking of translation interfaces, twin interfaces and mixed layer compounds;
- diffuse scattering from substitutionally ordering alloys with a column structure;
- diffraction contrast at defects. In particular the extinction rule based on the g·R criterion remains valid if the defect is parallel to the incident beam.

5.3. High resolution images

The wavefunction in the image plane can be written as the convolution product of the wavefunction at the exit face of the crystal with the impulse response function t(R) of the electron microscope

$$\Psi(\mathbf{R},z) = 1 + \sum_{i} \left[\exp\left\{-i\pi \frac{E_{i}}{E_{o}}kz\right\} - 1\right] \times C_{i}\Phi_{i}(\mathbf{R} - \mathbf{R}_{i}) * t(\mathbf{R}).$$
(27)

If the microscope is operated close to optimum focus and in axial mode, the impulse response function is sharply peaked.

If the distance between the columns is larger than the width of the impulse response function $t(\mathbf{R})$, the overlap between convolution products $\Phi_i * t(\mathbf{R})$ of adjacent sites can be assumed to be small so that each column is thus imaged separately. The contrast of a particular column varies periodically with thickness. The periodicity can be different for different types of columns. It is interesting to note that the functions Φ_i as well as $t(\mathbf{R})$ are symmetrical around the origin, provided the objective aperture is centred around the optical axis. Hence, the image of a column is rotationally symmetric around the position R_i of the columns. The intensity at R_i is a maximum or a minimum. The positions of the columns can thus be determined from the positions of the intensity extrema.

In case the resolution of the microscope is insufficient to discriminate the individual columns, or the focus is not close to optimum, the overlap between the convolution products of adjacent columns cannot be avoided and the interpretation of the contrast is not straightforward.

5.4. Direct structure retrieval

Using holographic methods such as sideband holography [9] or focus variation [10], it is possible to reconstruct the exit wave of an object. In order to retrieve the crystal structure out of this object wave one can use this channelling theory. Indeed, expression (23) yields a simple analytical expression for the wavefunction at the exit of a column in terms of Z, d and z. Albeit approximately, this expression is sufficiently simple to be used in a final least squares

fit from which these structural parameters can be obtained. If necessary, the residual imaging parameters such as $C_{\rm s}$ and defocus can be fitted simultaneously.

5.5. Other applications

The simple expressions (16) and (21) can also be used to study other observed effects related to scattering such as

- · dynamical extinction and extinction contours,
- · radiation damage at extinction contours,
- periodicity in Argand diagrams of diffracted heams.
- · periodicity in the image contrast in Quantitem,
- · Z contrast,
- · Alchemi,
- applicability of direct methods based on Sayre's equation.

6. Conclusion

The real-space channelling theory for isolated columns provides a simple and intuitive means to express the exact wavefunction of an object in terms of the projected column structure.

The theory is valid for most crystal thicknesses used in HREM situations. It provides a simple analytical tool to study dynamical scattering in a crystal and related effects and to solve the inverse problem of deducing the projected crystal structure out of the experimentally reconstructed exit wave.

Acknowledgements

D.V.D. wishes to thank J. Mayer, A. Skowron, R. Withers and C. Deininger for stimulating discussions. One of us (M.O.d.B.) is indebted to the Belgian NFWO for financial support.

References

- S. Amelinckx, G. Van Tendeloo and J. Van Landuyt, Bull. Mater. Sci. 6(3) (1984) 417.
- [2] D. Van Dyck, G. Van Tendeloo and S. Amelinckx, Ultramicroscopy 10 (1982) 263.

- [3] D. Van Dyck, in: Advances in Electronics and Electron Physics, Ed. P. Hawkes (Academic Press, New York, 1985).
- [4] J. Lindhard, Mat. Fys. Medd. Dan. Vidensk. Selsk. 34 (1965)
 1. A. Tamura and Y.K. Ohtsuki, Phys. Status Solidi (b) 73 (1974) 477. A. Tamura and F. Kawamura, Phys. Status Solidi (b) 77 (1976) 391. B. Buxton, J.E. Loveluck and J.W. Steeds, Phil. Mag. A 3 (1978) 259. C.J. Humphries and J.C.H. Spence, Proc. 37th Annu. EMSA Meeting, San Antonio, TX, 1979 (Claitor's, Baton Rouge, LO, 1979) p. 554.
- [5] D. Van Dyck, J. Danckaert, W. Coene, E. Selderslaghs, D. Broddin, J. Van Landuyt and S. Amelinckx, in: Computer Simulation of Electron Microscope Diffraction and Images, Eds. W. Krakow and M. O'Keefe (The Minerals, Metals and Materials Society, Warrendale, PA, 1989).

- [6] M.V. Berry and K.E. Mount, Rep. Progr. Phys. 35 (1972) 315.
- [7] K. Kambe, G. Lempfuhl and F. Fujimoto, Z. Naturforsch. 29a (1974) 1034. F. Fujimoto, Proc Vth Int. Conf. on High Voltage Electron Microscopy, Kyoto, 1977, p. 271.
- [8] D. Shindo and M. Hirabayashi, Acta Cryst. A 44 (1988) 954.
- [9] H. Lichte, Ultramicroscopy 64 (1996) 79 (this volume).
- [10] M. Op de Beeck, D. Van Dyck and W. Coene, Ultramicroscopy 64 (1996) 167 (this volume).
- [11] K. Matsuhata, D. Van Dyck., J. Van Landuyt and S. Amelinckx, Ultramicroscopy 13 (1984) 343.